

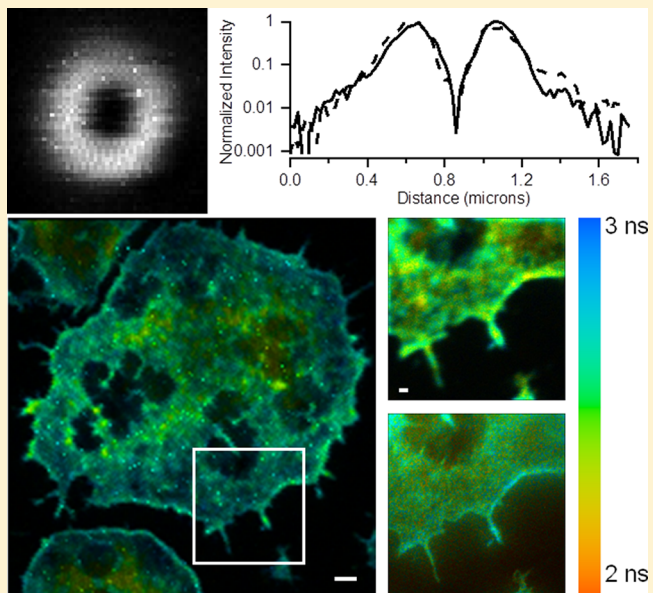
Supercontinuum Stimulated Emission Depletion Fluorescence Lifetime Imaging

Michael D. Lesoine,^{1,2} Sayantan Bose,¹ Jacob W. Petrich,^{*,1,2} and Emily A. Smith^{*,1,2}

¹U.S. Department of Energy, Ames Laboratory, Ames, Iowa 50011, United States

²Department of Chemistry, Iowa State University, 1605 Gilman Hall, Ames, Iowa 50011, United States

ABSTRACT: Supercontinuum (SC) stimulated emission depletion (STED) fluorescence lifetime imaging is demonstrated by using time-correlated single-photon counting (TCSPC) detection. The spatial resolution of the developed STED instrument was measured by imaging monodispersed 40-nm fluorescent beads and then determining their fwhm, and was 36 ± 9 and 40 ± 10 nm in the X and Y coordinates, respectively. The same beads measured by confocal microscopy were 450 ± 50 and 430 ± 30 nm, which is larger than the diffraction limit of light due to underfilling the microscope objective. Underfilling the objective and time gating the signal were necessary to achieve the stated STED spatial resolution. The same fluorescence lifetime (2.0 ± 0.1 ns) was measured for the fluorescent beads by using confocal or STED lifetime imaging. The instrument has been applied to study Alexa Fluor 594-phalloidin labeled F-actin-rich projections with dimensions smaller than the diffraction limit of light in cultured cells. Fluorescence lifetimes of the actin-rich projections range from 2.2 to 2.9 ns as measured by STED lifetime imaging.



INTRODUCTION

Diffraction limits traditional far-field optical microscopies to a lateral resolution of $\sim\lambda/2NA$, where λ is the wavelength of light and NA is the numerical aperture of the optical system.¹ The diffraction limit is greater than 200 nm with use of visible wavelengths. There are several optical imaging techniques that circumvent the diffraction limit and enable the study of phenomena that occur in subdiffraction spatial regimes. Stochastic techniques such as stochastic optical reconstruction microscopy (STORM) rely on turning a subset of fluorophores on and then off in combination with localization procedures.² Near-field techniques require a probe in close proximity to the sample, and may not be suitable for corrugated or sensitive samples.³ Hell and co-workers^{4–10} described and demonstrated the technique referred to as stimulated emission depletion (STED), whereby the diffraction-limited resolution in far-field fluorescence microscopy is circumvented by using point spread function engineering.

The basic operating principle of STED microscopy is inhibiting the fluorescence at the periphery of a diffraction-limited spot by stimulated emission. A tightly focused, scanning excitation laser pulse of tens-of-picoseconds duration and a toroid-shaped STED laser pulse of hundreds-of-picosecond duration are used. The STED pulse is shaped by phase modulation, and has zero intensity at its center. The stimulated

emission pulse depopulates the excited electronic states of the fluorophores within the toroidal beam profile, leaving a spot of excited fluorophores, which is smaller than the diffraction limit, at the center of the toroid. The net result enables signal collection from an excitation volume that is smaller than the dimensions set by diffraction. Resolution in the 15–20-nm range has been reported, with molecular-scale resolution fluorescence measurements fundamentally possible in the far-field.⁵ STED has been demonstrated by using various instrumental configurations. The use of pulsed lasers is well-suited to gating the fluorescence signal, while continuous-wave lasers simplify the instrumentation and are a cost-effective choice. Spatial light modulators or vortex phase plates are commonly used to generate the required STED toroid profile.^{7,9,11} Crucial to achieving optimum spatial resolution is the ability to obtain a minimum approaching zero in the toroid. STED microscopy with a supercontinuum (SC) laser to supply both the excitation and STED wavelengths simplifies instrument setup, and the wavelength tunability opens the possibility of using an increased range of dyes.^{11,12} A ~9-fold improve-

Received: April 23, 2012

Revised: June 11, 2012

Published: June 13, 2012

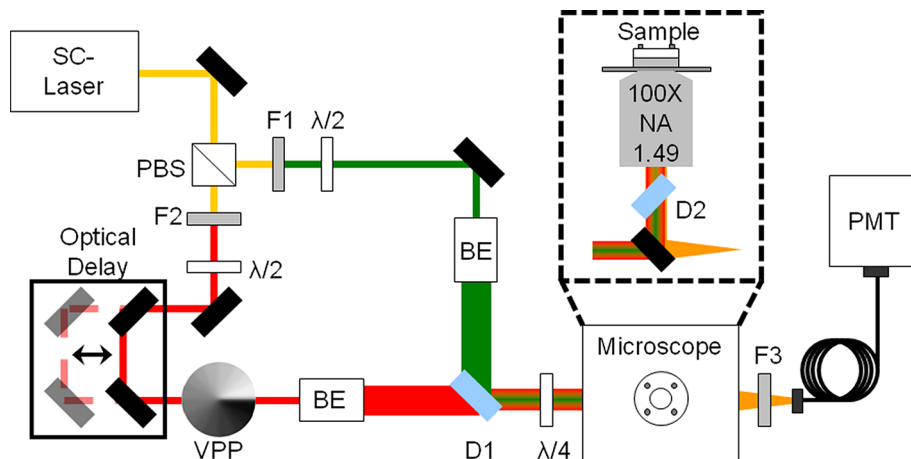


Figure 1. Schematic of the SC STED fluorescence lifetime microscope showing the SC being split into two paths by a polarizing beam splitter (PBS). The desired wavelengths are extracted by interference filters (F), F1 and F2, which isolate the excitation and STED wavelengths, respectively. Both paths have half-wave plates ($\lambda/2$) for adjusting the polarization. The STED path has an optical delay line to adjust the arrival of the pulses at the sample and the toroid shape is imparted by using a vortex-phase plate (VPP). Both beams are expanded and collimated by using beam expanders (BE) and recombined by using a long-pass dichroic (D1). A quarter-wave plate ($\lambda/4$) generates circular polarization. The beams are reflected to the sample with a dichroic mirror (D2) that transmits the resulting fluorescence to the emission filters (F3). The fluorescence is then passed onto a multimode fiber (MMF) and detected by a photomultiplier tube (PMT). The portion of the schematic within the dashed lines presents a view perpendicular to the laser table.

ment in the lateral (i.e., in the focal plane) spatial resolution has been reported with SC STED microscopy.^{11,13}

Besides obtaining subdiffraction resolution images, STED can be coupled with fluorescence-lifetime imaging microscopy (FLIM) to perform time-resolved experiments^{12,14} and to acquire lifetime images. Time-gating the signal has been shown to improve signal-to-background values noticeably and also to improve the spatial resolution.¹² Time-gating improves the lateral resolution by selectively rejecting photons from signal not originating from the center of the toroid. To date, a few groups have used TCSPC in STED experiments, but have not exploited the ability of this photon-counting technique to obtain kinetic data from subdiffraction spots.^{12,14,15} Hell and co-workers have, however, used lifetimes obtained from TCSPC to distinguish different fluorophores.¹⁴ Fluorescence lifetime measurements provide details about molecular dynamics and molecular environments, and when combined with STED can reveal information about local environments on the tens-of-nanometer scale. Herein, SC STED fluorescence lifetime microscopy is demonstrated and tested by using two very different systems: monodispersed, fluorescent beads and Alexa Fluor 594-phalloidin labeled actin fibers in cultured cells. The data show that high-quality fluorescence lifetime data can be obtained in subdiffraction spots as small as 36–40 nm in diameter.

MATERIALS AND METHODS

Instrumentation. Figure 1 shows a schematic of the home-built STED microscope that uses a SC laser (SC-450-pp-he, Fianium, Southampton, UK) for the excitation and STED pulses, which ensures that both pulses are inherently synchronized. A 2-MHz repetition rate is used to limit photobleaching of the fluorophore. The energies of the excitation and STED pulses are 1 pJ and 4 nJ, as measured before the microscope objective. The instrument response functions for the excitation and STED pulses are 90 and 150 ps, respectively, as measured by the traditional method of monitoring the profile obtained from light scattered from a

suspension of nonfluorescent nondairy creamer in water. Dielectric mirrors are used in the beam paths (10Q20BB.1, Newport, Irvine, CA) to remove the infrared wavelengths from the SC.

The laser output is initially split by using a polarizing beam splitter (PBS201, Thorlabs, Newton, New Jersey). Band-pass filters isolate the desired wavelengths for the excitation (570 ± 5 nm, product ZS70/10X, Chroma, Bellows Falls, VT) and STED beams (695 ± 10 nm, product D695/20, Chroma). Half-wave plates (AHWP05M-600, Thorlabs) are used in both beam paths to ensure matching polarizations. The toroidal STED beam is generated by using a vortex phase plate (RPC Photonics, Rochester, NY), which attenuates the intensity at the center of the beam profile by 99.7% (Figure 2). An optical delay line is also added to the STED path to ensure the desired temporal profile of the excitation and STED pulses, where the latter precedes the excitation pulse with a peak-to-peak difference of ~80 ps. The STED pulse needs to lag behind the excitation pulse enough to allow the latter to populate the

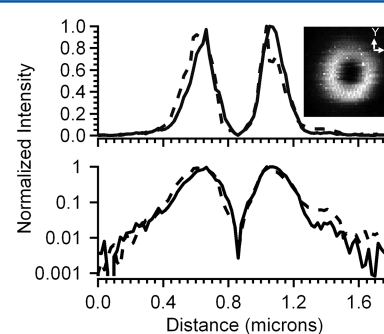


Figure 2. Orthogonal cross sections of the toroidal STED beam profile (X-coordinate solid line, Y-coordinate dotted line) on a linear (top) and log scale (bottom). The log plot reveals an intensity drop in the center of the profile to ~0.3% of the maximum intensity. The inset image was obtained by measuring the scatter from 60-nm gold nanoparticles.

excited state, before the arrival of the STED pulse. The STED beam profile was measured as previously reported.¹⁶ Beam expanders are used in both the excitation and STED paths to adjust the beam size and spatially filter the beam. The beams are recombined with a dichroic mirror (ZT594RDC, Chroma). A quarter-wave plate (AQWP05M-600, Thorlabs) placed before the microscope generates circular polarization, which has been previously shown to optimize the STED signal.¹⁷

The collinear pulses are directed to a microscope (Eclipse Ti, Nikon, Melville, NY) objective (CFI Apo TIRF 100x, 1.49 NA, Nikon) with use of a dichroic mirror (635-70BPDC, Chroma) that reflects both the excitation and STED wavelengths while allowing transmission of the resulting fluorescence. The excitation pulse slightly underfills the objective to minimize artifacts in the periphery of the excitation pulse that deteriorate image quality at higher STED powers.¹⁸ The fluorescence signal is directed to the detection path containing stacked emission filters (FF01-629/56-25, Semrock, Rochester, NY) and a multimode fiber (Thorlabs) coupled to a hybrid PMT (HPM-100-40, Becker and Hickl, Berlin, Germany). The PMT is linked to a single-photon counting card (SPC-830, Becker and Hickl) that allows for both intensity and lifetime measurements.

Sample Preparation. The instrument's spatial resolution was measured with use of monodispersed fluorescent beads, prepared by attaching carboxylate modified fluorescent beads (FluoSpheres red, 40 nm, Invitrogen, Grand Island, NY) to a lysine-coated glass coverslip (474030-9000-000, Carl Zeiss Microscopy, Thornwood, NY).¹⁹ These samples were embedded (VECTASHIELD Hardest Mounting Medium, Burlingame, CA), covered with a coverslip, and left to dry for 30 min before imaging.

Details of the cultured *Drosophila* S2 cells used in this study and their propagation have been previously described.²⁰ A 50- μ L solution of cells (1.5×10^6 cells/mL) was allowed to spread on a glass substrate for 1 h, followed by removing unspread cells with phosphate buffered saline (PBS) rinses. The cells were fixed with 4% paraformaldehyde for 10 min, then rinsed with PBS. Cells were permeabilized with a 0.1% Triton X-100 solution in PBS for 2 min and rinsed with PBS followed by a 1% bovine serum albumin solution in PBS to prevent nonspecific binding of the Alexa Fluor 594-phalloidin to the glass. A 50- μ g/mL solution of Alexa Fluor 594-phalloidin was used to stain the cells for 6 h. After being rinsed with PBS, the cells were embedded as described above.

Imaging. Images were generated by raster scanning the sample over the beams, using a piezo stage (Nano-PDQ375, Mad City Laboratories, Madison, WI) that has subnanometer accuracy. Data were collected with use of the Single Photon Counter v9.30 software (Becker and Hickl) and further analyzed by using SPCImage (Becker and Hickl). All of the TCSPC measurements were made in a ~ 8 ns time window with a total of 64 channels, and a 5-ms collection time per pixel to obtain sufficient counts for determining and resolving the lifetime data. The pixel size was 19.5 nm over a 256×256 or 512×512 pixel scan area, unless otherwise noted. Because stimulated emission is not complete at early times, the initial 0.5 ns of the fluorescence decay traces were discarded prior to fitting them with a single exponential. All measurements were performed at room temperature. Cross sections showing fluorescence intensity of a line of adjacent pixels were generated with Image-J 1.44p (National Institutes of Health, USA), and

all subsequent data processing was performed with Origin (OriginLab, Northampton, MA).

RESULTS AND DISCUSSION

Instrumental Spatial Resolution: Fluorescent Beads.

The system's spatial resolution was measured by scanning 40-nm fluorescent beads immobilized on a coverslip with confocal (excitation beam with STED beam blocked) or STED (excitation and STED beams) illumination. Figure 3 presents

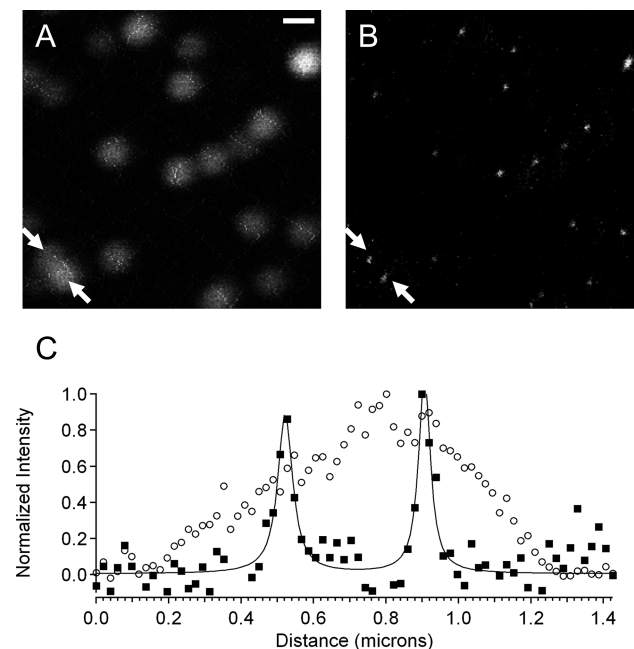


Figure 3. Confocal (A) and STED (B) fluorescence intensity images of 40-nm fluorescent beads. The white arrows highlight two beads that are unresolved in the confocal image but resolved with STED. (C) The STED cross section (solid squares) fit to a Lorentzian yields a fwhm of 49 and 39 nm. The confocal cross section (open circles) was not fit. The scale bar represents 500 nm and is the same for both images.

confocal (A) and STED (B) images of the fluorescent beads. Cross sections of fluorescence intensity (Figure 3C) taken from the region shown with white arrows in the images indicate there is an improvement in the spatial resolution measured by STED. Two fluorescent beads are merged into one feature in the confocal image, but are resolved in the STED cross section. The STED cross sections were fit to a Lorentzian, for which there is precedent in the literature.^{15,21} The fwhms were 49 and 39 nm for the left and right bead, respectively.

Table 1 shows the fwhm obtained by fitting the X- and Y-fluorescence intensity cross sections of 15 beads with confocal or STED illumination. For the confocal images, the average fwhm are 450 ± 50 and 430 ± 30 nm. These values are larger than expected for the diffraction limit (~ 280 nm) for this system for two reasons: the objective is slightly underfilled and there is an index of refraction mismatch at the sample interface arising from the embedding medium. Underfilling the objective was required to minimize excitation artifacts that are otherwise prominent in the STED images. The embedding medium enables the use of the microscope's autofocus function, which ensures that the focus is maintained over long scan times. Unlike the STED cross sections, which seem to be well-

Table 1. Full Width Half Maximum (fwhm) Values Obtained from X- and Y-Cross Sections of Fluorescent Beads Obtained in the Image Shown in Figure 3, or Similar Images

fluorescent beads	confocal		STED	
	X fwhm (nm)	Y fwhm (nm)	X fwhm (nm)	Y fwhm (nm)
1	504	451	39	33
2	484	448	41	55
3	454	468	52	39
4	561	412	33	22
5	462	415	33	35
6	408	411	54	45
7	435	400	34	46
8	450	452	43	20
9	398	457	33	27
10	451	400	27	44
11	441	429	37	78
12	355	376	41	52
13	514	486	26	41
14	382	410	31	42
15	480	427	23	57
average	450 ± 50	430 ± 30	36 ± 9	40 ± 10

represented by Lorentzians, the confocal intensity distributions are better described by Gaussians.

The average fwhms of the STED cross sections for 15 beads are 36 ± 9 nm for the X-coordinate and 40 ± 10 nm for the Y-coordinate (Table 1). The small difference in the X and Y spatial resolution is due to subtle differences in the STED profile (Figure 2). The above resolution is achieved by time-gating the signal. A 0.5-ns gate provided the best spatial resolution. Without time-gating, the average fwhm of the beads was 80 nm. (Using a gate longer than 0.5 ns resulted in an apparent worsening of the spatial resolution, most likely owing to a reduction of the signal-to-noise ratio accompanying the detection of a reduced amount of fluorescence.) Time-gating also reduced the background and improved the uncertainty of the measurement, as obtained from the full-width at half-maximum of the cross section of the beads. The uncertainty decreased from 44% without gating the signal to 26% with gating.

SC STED Fluorescence Lifetime Imaging. Fluorescence lifetime images acquired from confocal and STED illumination, and their representative decay curves, are given for the 40-nm fluorescent bead sample in Figure 4. The main challenge to obtaining fluorescence lifetimes by using STED is a \sim 200-fold drop in the probed volume compared to confocal imaging. There would be \sim 200 molecules in the confocal probe volume assuming a homogeneous 1- μ M solution compared to 1 molecule in the STED probe volume. Hell and co-workers previously reported an increase in the collection time per pixel from 1 ms for intensity images to 3 ms for TCSPC detection.¹⁴ The longer collection time is required to acquire sufficient counts in the fluorescence decay traces, and to obtain a reliable fit. Theoretically \sim 185 photons in the peak channel are necessary to resolve an exponential decay of single molecules in solution.²² On the other hand, Xie and co-workers resolved two exponentials in single molecule fluorescence decay traces with 64 counts in the peak channel.²³ It is noteworthy that the collection time cannot be increased significantly, because longer exposure of the fluorophores causes photobleaching. A similar issue is encountered when attempting finer movement of the

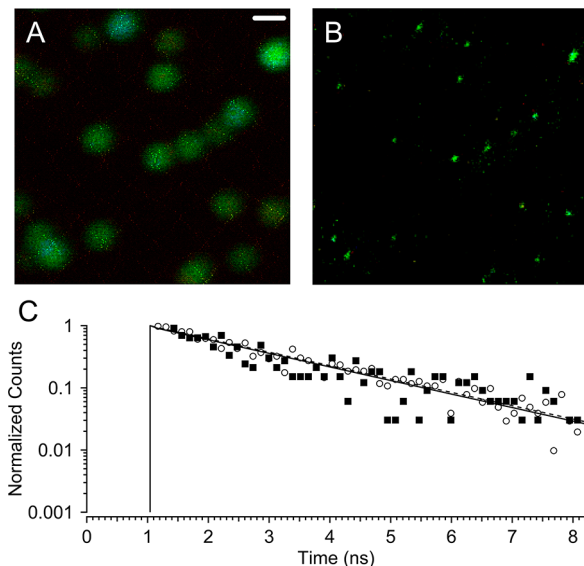


Figure 4. Confocal (A) and STED (B) fluorescence lifetime images of 40-nm fluorescent beads. Representative fluorescence decay curves (C) for the confocal (open circles, solid fit) and STED (solid squares, dashed fit) were fit to a single exponential with a 2.0 ± 0.1 ns fluorescence lifetime. The scale bar represents 500 nm and is the same for both images.

sample stage. We thus scan a region once with only the excitation beam and then a second time with both the excitation and STED beams. Considering the trade-off between collection time and photobleaching rate, we chose to use a 5-ms collection time per pixel, which not only provided 50–100 counts in the peak channel to resolve exponential decays, but also prevented the fluorophores from extensively photo-bleaching. The confocal (A) and STED (B) lifetime images reveal a homogeneous lifetime distribution, which is expected given the similar size of the fluorescent beads and the spatial resolution obtained with STED illumination. The fluorescence lifetime of the beads (2.0 ± 0.1 ns) obtained from confocal and STED illumination is identical within the uncertainty of the measurement, as shown in Figure 4C. This indicates that the STED beam does not perturb the lifetime measurement, even with time gating.

Subdiffraction Fluorescence Lifetime Imaging of Cultured Cells. STED fluorescence lifetime imaging was applied to F-actin in cultured cells. The protein, actin, is in monomeric (G actin) and filamentous (F actin) forms within the cell; and proper function of the actin cytoskeleton is important for most basic cellular functions. F-actin can be found in cellular structures that are smaller than the diffraction limit of light,²⁴ and traditional far-field imaging techniques provide few details of these structures. The small molecule, phalloidin, binds with high specificity to F-actin.²⁵ With a Alexa Fluor 594 fluorophore conjugated to phalloidin it is possible to visualize the distribution of F-actin in the cell. STED microscopy (intensity images) has been previously applied to measure actin fibers in cultured cells with 100-nm resolution.²⁶ A confocal intensity image of a whole cultured cell labeled with Alexa Fluor 594-phalloidin is shown in Figure 5A. Several F-actin structures are visible in the cell, including actin-rich projections around the periphery of the cell. An expanded view of two projections is shown with confocal (Figure 5B) and STED (Figure 5C) illumination. The images and the

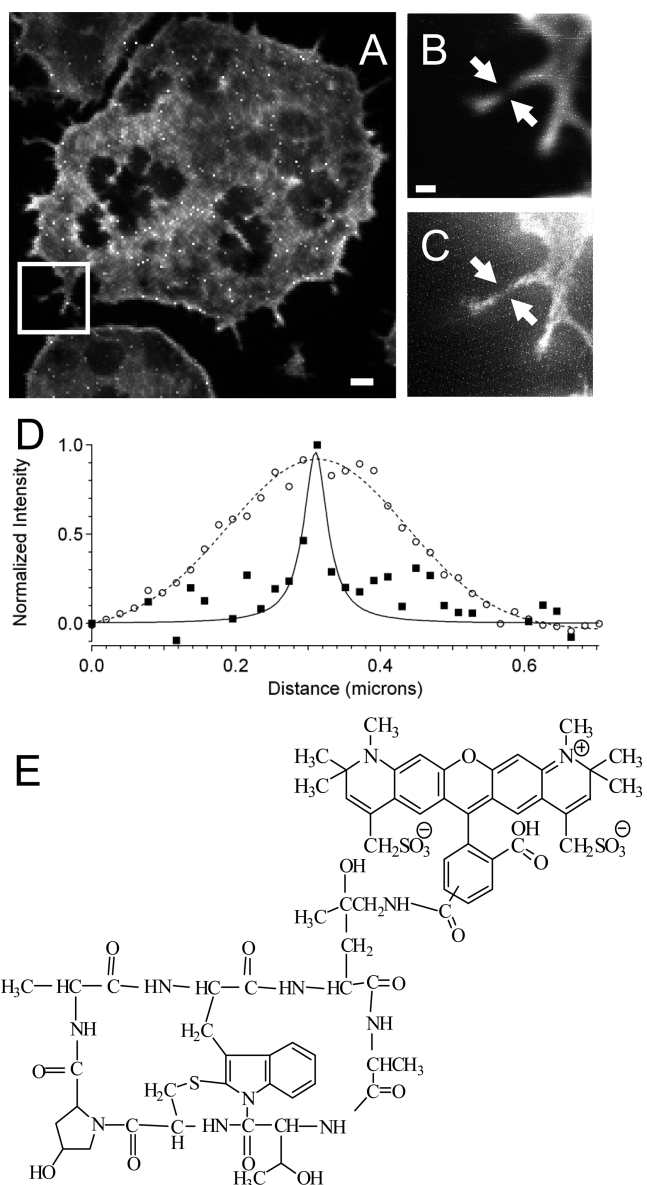


Figure 5. Fluorescence intensity images of a cell with Alexa Fluor 594-phalloidin labeled actin. (A) An overview confocal image with an ~195-nm pixel size, scale bar of 2 μm . (B) Confocal and (C) STED images of a selected $5 \times 5 \mu\text{m}^2$ region shown with a white box in part A. Scale bars for parts B and C represent 500 nm. The arrows in parts B and C represent the cross sections shown in part D for the confocal (open circles) and STED (solid squares) images. The fwhms from the Gaussian (confocal) and Lorentzian (STED) fits are 290 and 38 nm, respectively. (E) Structure of Alexa Fluor 594-phalloidin.

corresponding cross sections (Figure 5D) of the narrowest point in one projection has the expected improvement in the STED spatial resolution. The fwhm of the confocal cross section is 290 nm and the same location measures 38 nm by STED.

Differences in the local actin environment could be measured as a distribution of the lifetimes for the fluorophore conjugated to F-actin bound phalloidin. A confocal fluorescence lifetime image of the entire cell (Figure 6A) was obtained in order to choose a specific region of interest for which to compare confocal lifetime images (Figure 6B) with STED lifetime images (Figure 6C). As with the intensity-based comparison presented in Figure 5, the STED fluorescence lifetime image of

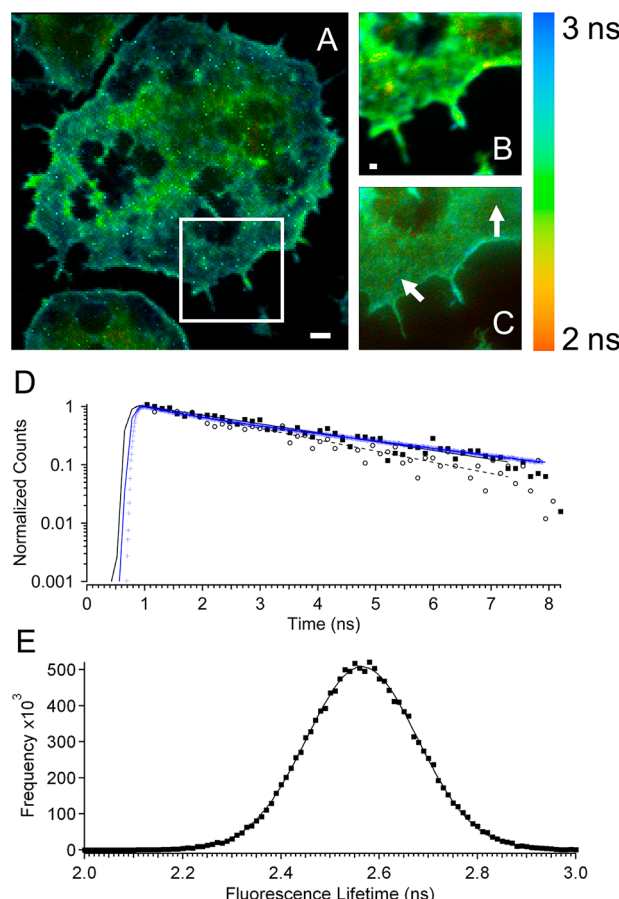


Figure 6. Fluorescence lifetime images of a cell with Alexa Fluor 594-phalloidin labeled actin. (A) An overview confocal image, \sim 195-nm pixel size, scale bar of 2 μm . (B) Confocal and (C) STED images of a selected $10 \times 10 \mu\text{m}^2$ region shown with a white box in part A. Scale bars for parts B and C represent 500 nm. (D) Representative fluorescence decay curves from two different regions (denoted by white arrows) from the image (part C) fit to a single exponential with 2.9-ns (solid square) or 2.2-ns (open circle) fluorescence lifetimes. For purposes of comparison, the fluorescence decay profile (blue) obtained from the Alexa Fluor 594-phalloidin conjugate, in the same medium used to prepare the cells, is presented in panel D. It is superposed over and is, within experimental error, identical with the 2.9-ns value obtained from the STED measurement. (E) A histogram of the STED fluorescence lifetime distribution from part C. The distribution of lifetimes obtained from the STED and confocal images are both well fit to Gaussians. The STED distribution has a mean of 2.6 ± 0.1 ns, and the confocal distribution has a mean of 2.55 ± 0.08 ns.

the region of interest reveals F-actin structural details that are blurred due to the diffraction limit in the confocal lifetime image. The fluorescence decay curves obtained from two locations from the STED image, indicated with white arrows, are presented in Figure 6D. These decay curves correspond to lifetimes of ~ 2.9 and ~ 2.2 ns. It is well-known that fluorescein-type dyes (e.g., ATTO, Alexa Fluor) are strongly quenched by tryptophan due to photoinduced electron transfer from tryptophan (which acts as a donor) to the fluorescein moiety (which acts as an acceptor).^{27,28} We note, however, that in a cell, because of its inherent complexity, tryptophan may be one of the quenchers of Alexa Fluor 594; but it is not necessarily the only one.

For purposes of comparison, the fluorescence decay profile obtained from the Alexa Fluor 594-phalloidin conjugate in the same medium used to prepare the cells is presented in Figure 6D. This profile was obtained with the same instrumentation used to obtain the STED lifetimes and an excitation wavelength of 570 nm. It can be superposed over the 2.9-ns STED profile; and this suggests that the 2.9-ns lifetime arises from unquenched fluorescent marker and that the difference in the STED lifetimes from one site to another in the cells may be attributed to the differential quenching of the Alexa Fluor 594 fluorescence by neighboring tryptophan residues and possibly other unknown species. The histogram (Figure 6E) of fluorescence lifetimes measured for every pixel in the STED image is well fit to a Gaussian.

As noted above, the decay curves obtained from the STED measurement that are presented in Figure 6D correspond to lifetimes of ~ 2.9 and ~ 2.2 ns, which we attribute to specific quenching interactions between Alexa Fluor and components of the cell. Because the data from Figure 6 represent only one measurement of one cell, means and associated errors could not be directly obtained for the lifetimes we cite. In order to obtain an estimate, we measured a solution of ATTO 590 in ethanol using the STED instrument. The data collected from 4096 pixels yielded a lifetime of 3.56 ± 0.06 ns, i.e., an error of about 2%. It is a reasonable assumption that the percent error for the STED-obtained Alexa Fluor 594-phalloidin lifetimes is similar. Even assuming an uncertainty of 10% for each lifetime, ~ 2.9 and ~ 2.2 ns lifetimes would be distinguishable from each other. Finally, in the interest of completeness, we present an alternate interpretation for the origin of the different lifetimes. The observation of a distribution of Alexa Fluor lifetimes that is very well described by a Gaussian (Figure 6E) could suggest that the spread in lifetimes merely reflects statistical error in measuring the fluorescent probe in different parts of the cell.

CONCLUSIONS

Fluorescence lifetime images with ~ 40 -nm lateral spatial resolution have been reported. Fluorescence lifetimes were statistically similar in confocal and STED measurements for both fluorescent beads and Alexa Fluor 594-phalloidin in cultured cells, and suggest a level of Alexa Fluor 594 quenching in cultured cells. These results open the door to measurements of lifetimes in heterogeneous domains smaller than the diffraction limit.

AUTHOR INFORMATION

Corresponding Author

*E-mail: jwp@iastate.edu (J.W.P.); esmith1@iastate.edu (E.A.S.).

Notes

The authors declare no competing financial interest.

ACKNOWLEDGMENTS

This research is supported by the U.S. Department of Energy, Office of Basic Energy Sciences, Division of Chemical Sciences, Geosciences, and Biosciences through the Ames Laboratory. The Ames Laboratory is operated for the U.S. Department of Energy by Iowa State University under Contract No. DE-AC02-07CH11358. The SC STED fluorescence lifetime microscope was built with equipment funds from the National Science Foundation Chemical Research Instrumentation and Facilities program (CHE-0845236). We thank Mr. Ujjal

Bhattacharjee, Dr. Suzanne Sander, and Dr. Kristopher J. McKee for technical assistance.

REFERENCES

- (1) Abbe, E. *Arch. Mikrosk. Anat.* **1873**, *9*, 413.
- (2) Rust, M. J.; Bates, M.; Zhuang, X. *Nat. Meth.* **2006**, *3*, 793.
- (3) Binnig, G.; Quate, C. F.; Gerber, C. *Phys. Rev. Lett.* **1986**, *56*, 930.
- (4) Hell, S. W.; Wichmann, J. *Opt. Lett.* **1994**, *19*, 780.
- (5) Donnert, G.; Keller, J.; Medda, R.; Andrei, M. A.; Rizzoli, S. O.; Lahrman, R.; Jahn, R.; Eggeling, C.; Hell, S. W. *Proc. Natl. Acad. Sci.* **2006**, *103*, 11440.
- (6) Klar, T. A.; Engel, E.; Hell, S. W. *Phys. Rev. E* **2001**, *64*, 066613.
- (7) Klar, T. A.; Hell, S. W. *Opt. Lett.* **1999**, *24*, 954.
- (8) Rittweger, E.; Han, K. Y.; Irvine, S. E.; Eggeling, C.; Hell, S. W. *Nat. Photon* **2009**, *3*, 144.
- (9) Willig, K. I.; Harke, B.; Medda, R.; Hell, S. W. *Nat. Meth.* **2007**, *4*, 915.
- (10) Willig, K. I.; Keller, J.; Bossi, M.; Hell, S. W. *New J. Phys.* **2006**, *8*, 106.
- (11) Wildanger, D.; Rittweger, E.; Kastrup, L.; Hell, S. W. *Opt. Express* **2008**, *16*, 9614.
- (12) Auksorius, E.; Boruah, B. R.; Dunsby, C.; Lanigan, P. M. P.; Kennedy, G.; Neil, M. A. A.; French, P. M. W. *Opt. Lett.* **2008**, *33*, 113.
- (13) Wildanger, D.; Medda, R.; Kastrup, L.; Hell, S. W. *J. Microsc.* **2009**, *236*, 35.
- (14) Bückers, J.; Wildanger, D.; Vicidomini, G.; Kastrup, L.; Hell, S. W. *Opt. Express* **2011**, *19*, 3130.
- (15) Vicidomini, G.; Moneron, G.; Han, K. Y.; Westphal, V.; Ta, H.; Reuss, M.; Engelhardt, J.; Eggeling, C.; Hell, S. W. *Nat. Meth.* **2011**, *8*, 571.
- (16) Schrader, M.; Hell, S. W. *J. Microsc.* **1996**, *184*, 143.
- (17) Dedecker, P.; Muls, B.; Hofkens, J.; Enderlein, J.; Hotta, J.-i. *Opt. Express* **2007**, *15*, 3372.
- (18) Leutenegger, M.; Eggeling, C.; Hell, S. W. *Opt. Express* **2010**, *18*, 26417.
- (19) Wurm, C. A.; Neumann, D.; Schmidt, R.; Egner, A.; Jakobs, S. Sample Preparation for STED Microscopy. In *Live Cell Imaging*, 2009, *591*, 185.
- (20) Dibya, D.; Arora, N.; Smith, E. A. *Biophys. J.* **2010**, *99*, 853.
- (21) Fitzpatrick, J. A. J.; Yan, Q.; Sieber, J. J.; Dyba, M.; Schwarz, U.; Szent-Gyorgyi, C.; Woolford, C. A.; Berget, P. B.; Waggoner, A. S.; Bruchez, M. P. *Bioconjugate Chem.* **2009**, *20*, 1843.
- (22) Köllner, M.; Wolfrum, J. *Chem. Phys. Lett.* **1992**, *200*, 199.
- (23) Dunn, R.; Holtom, G.; Mets, L.; Xie, X. *J. Phys. Chem.* **1994**, *98*, 3094.
- (24) Fuchs, E.; Cleveland, D. W. *Science* **1998**, *279*, 514.
- (25) Lengsfeld, A. M.; Löw, I.; Wieland, T.; Dancker, P.; Hasselbach, W. *Proc. Natl. Acad. Sci.* **1974**, *71*, 2803.
- (26) Farahani, J.; Schibler, M.; Bentolila, L. Stimulated Emission Depletion (STED) Microscopy: from Theory to Practice. In *Microscopy: Science, Technology, Applications and Education*; Méndez-Vilas, A., Díaz, J., Eds.; Formatax Research Center: Badajoz, Spain, 2010; Vol. 2, p 1539.
- (27) Chen, H.; Ahsan, S.; Santiago-Berrios, M.; Abruña, H.; Webb, W. *J. Am. Chem. Soc.* **2010**, *132*, 7244.
- (28) Marmé, N.; Knemeyer, J.-P.; Sauer, M.; Wolfrum, J. *Bioconjugate Chem.* **2003**, *14*, 1133.